CellPress
PARTNER JOURNAL

Molecular Plant
Research Article

Protomer Roles in Chloroplast Chaperonin Assembly and Function

Cuicui Bai[1,3,5], Peng Guo[1,3,5], Qian Zhao[1,3], Zongyang Lv[1], Shijia Zhang[1,3], Fei Gao[1], Liyan Gao[2], Yingchun Wang[2], Zhixi Tian[1], Jifeng Wang[4], Fuquan Yang[4] and Cuimin Liu[1,*]

[1]State Key Laboratory of Plant Cell and Chromosome Engineering, Institute of Genetics and Developmental Biology, Chinese Academy of Sciences, Beijing 100101, China

[2]Key Laboratory of Molecular Development Biology, Institute of Genetics and Developmental Biology, Chinese Academy of Sciences, Beijing 100101, China

[3]University of Chinese Academy of Sciences, Beijing 100101, China

[4]Laboratory of Protein and Peptide Pharmaceuticals and Laboratory of Proteomics, Institute of Biophysics, Chinese Academy of Sciences, Beijing 100101, China

[5]These authors contributed equally to this article.

***Correspondence: Cuimin Liu (cmliu@genetics.ac.cn)**

http://dx.doi.org/10.1016/j.molp.2015.06.002

ABSTRACT

The individual roles of three chloroplast CPN60 protomers (CPN60α, CPN60β1, and CPN60β2) and whether and how they are assembled into functional chaperonin complexes are investigated in *Chlamydomonas reinhardtii*. Protein complexes containing all three potential subunits were identified in *Chlamydomonas*, and their co-expression in *Escherichia coli* yielded a homogeneous population of oligomers containing all three subunits (CPN60αβ1β2), with a molecular weight consistent with a tetradecameric structure. While homo-oligomers of CPN60β could form, they were dramatically reduced when CPN60α was present and homo-oligomers of CPN60β2 were readily changed into hetero-oligomers in the presence of ATP and other protomers. ATP hydrolysis caused CPN60 oligomers to disassemble and drove the purified protomers to reconstitute oligomers *in vitro*, suggesting that the dynamic nature of CPN60 oligomers is dependent on ATP. Only hetero-oligomeric CPN60αβ1β2, containing CPN60α, CPN60β1, and CPN60β2 subunits in a 5:6:3 ratio, cooperated functionally with GroES. The combination of CPN60α and CPN60β subunits, but not the individual subunits alone, complemented GroEL function in *E. coli* with subunit recognition specificity. Down-regulation of the CPN60α subunit in *Chlamydomonas* resulted in a slow growth defect and an inability to grow autotrophically, indicating the essential role of CPN60α *in vivo*.

Key words: chaperonin, Cpn60, photosynthesis, protomer, assembly

Bai C., Guo P., Zhao Q., Lv Z., Zhang S., Gao F., Gao L., Wang Y., Tian Z., Wang J., Yang F., and Liu C. (2015). Protomer Roles in Chloroplast Chaperonin Assembly and Function. Mol. Plant. **8**, 1478–1492.

INTRODUCTION

Most proteins reach their functionally native state spontaneously after emerging from the ribosome, but a minority of proteins require the assistance of chaperones to fold. Chaperones are essential for maintaining cellular protein homeostasis and exist in all kingdoms of life (Hartl et al., 2011). The chaperonin system is a well-studied chaperone family with a cylindrically shaped structure containing 14–16 subunits that form two back-to-back stacked rings (Xu et al., 1997; Leitner et al., 2012). Each ring contains a central cavity where folding and refolding of a wide variety of newly synthesized or stress-denatured polypeptides occur.

Chaperonins are divided into two related, but distinct groups; group I chaperonins are found in prokaryotes (e.g. GroEL in *Escherichia coli*) and eukaryotic organelles including mitochondria (Hsp60) and chloroplasts (Cpn60), and group II chaperonins exist in Archaea (thermosome) and the eukaryotic cytosol (TriC/CCT) (Kim et al., 1994; Horwich et al., 2007). The most distinct difference between the two groups is the dependence on co-chaperonins (Hsp10 family). Hsp10 co-chaperonins form homo-heptameric rings that function as detachable lids binding to the ends of the group I chaperonin cylinders to form isolated environments for protein folding (Horwich et al., 2006), whereas group II chaperonin subunits carry flexible protrusions that extend from the apical domains that act as built-in lids to form the cavity for folding the nascent polypeptides (Booth et al., 2008).

Chloroplast chaperonin Cpn60 (originally named Rubisco binding protein [Hemmingsen and Ellis, 1986]) was suggested to mediate

Published by the Molecular Plant Shanghai Editorial Office in association with Cell Press, an imprint of Elsevier Inc., on behalf of CSPB and IPPE, SIBS, CAS.

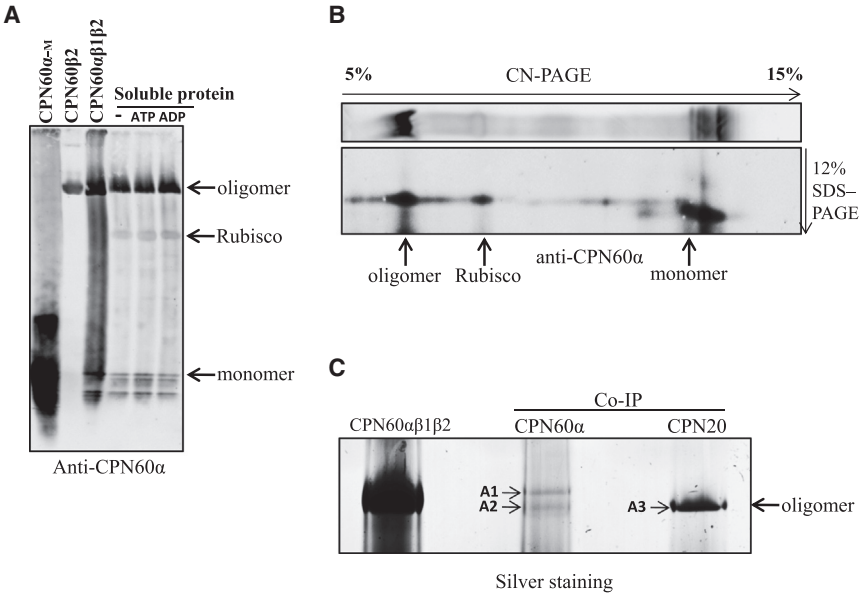

Figure 1. Oligomeric States and Composition of CPN60 Oligomers *In Vivo*.

(A) Analysis of the oligomeric states of CPN60 subunits *in vivo* by colorless native (CN) PAGE. Recombinantly purified monomeric CPN60α_{-M}, oligomeric CPN60β2, and CPN60αβ1β2 were loaded as controls. *Chlamydomonas* total soluble proteins were supplied with an ATP regenerating system (2 mM ATP, 10 U of creatine kinase, and 10 mM phosphocreatine) or had ATP converted into ADP by 2 mM ADP, 10 U of hexokinase, and 10 mM glucose after carbonyl cyanide p-trifluoromethoxyphenylhydrazone treatment. The proteins were then separated on a 5%–13% colorless native PAGE, transferred directly to nitrocellulose membranes, and immunodetected with serum against CPN60α.

(B) Soluble proteins from *Chlamydomonas* were separated using a 5%–13% colorless native PAGE (top gel) and separated in the second dimension on a 12% SDS–PAGE and then transferred to nitrocellulose (bottom gel). Proteins were immunodetected with antibodies against CPN60α.

(C) Soluble extract from *Chlamydomonas* cells was incubated with protein A–Sepharose coupled to either anti-CPN60α or anti-CPN20 serum. Precipitated proteins were eluted from antibodies by incubation with excess recombinant purified CPN60α or CPN20 overnight at 4°C. Eluted proteins were separated using 6% mini-native PAGE and visualized by silver staining. The CPN60 oligomers were marked as A1–A3 for identification by mass spectrometry. Co-IP, Co-immunoprecipitation.

the folding of newly synthesized plant hexadecameric Rubisco. Purified chaperonin from plants is thought to contain equal amounts of Cpn60α and Cpn60β (Cpn60$\alpha_7\beta_7$) (Hemmingsen and Ellis, 1986; Martel et al., 1990; Bonk et al., 1996). In contrast, two types of oligomers were obtained upon *in vitro* reconstitution: one composed of homo-tetradecameric Cpn60β subunits and the other consisted of both subunit types (Dickson et al., 2000; Vitlin et al., 2011). The existence of multiple chloroplast *Cpn60* genes in individual genomes (e.g. six genes in *Arabidopsis thaliana* [Hill and Hemmingsen, 2001] and three genes in *Chlamydomonas reinhardtii* [Schroda, 2004]) makes it difficult to predict the composition and arrangement of Cpn60 oligomers. Two distinct Cpn60 oligomers from plant stroma extract were obtained, which suggested that at least two types of chaperonins exist in plastids (Nishio et al., 1999). Suzuki et al. (2009) showed that two types of Cpn60β and one Cpn60α are important for chloroplast biogenesis, suggesting that these three may work together. Furthermore, Cpn60β4 formed a hetero-oligomer with Cpn60α1 and the other three Cpn60β subunits in *Arabidopsis thaliana*, supporting a hetero-oligomeric composition of Cpn60 complexes in chloroplasts (Peng et al., 2011). In *Arabidopsis*, the DNA insertion mutant of either Cpn60α subunit is lethal, suggesting that α type subunits do not have functional redundancy, while two Cpn60β subunits were functionally redundant and Cpn60β4 was specifically required to fold certain substrates (Suzuki et al., 2009; Peng et al., 2011). Presently, subunit composition and the individual role of protomers in functional chloroplast chaperonin oligomers are still debated.

Chlamydomonas contains three chloroplast CPN60 subunits, CPN60α, CPN60β1, and CPN60β2, and three potential chaperonin co-factor subunits, CPN23, CPN20, and CPN11. Here, we present an in-depth analysis of the subunit composition of CPN60 oligomers from *Chlamydomonas* chloroplasts, as well as the functional roles of CPN60 subunits within these oligomers. Chloroplast complexes isolated from *Chlamydomonas* contained all three subunits (CPN60αβ1β2). The composition of functional CPN60 oligomers was investigated *in vitro*. Disassembly of oligomers, specific to chloroplast CPN60, was triggered by ATP hydrolysis, whereas ATP also drove the reconstitution of CPN60 oligomers, a process in which CPN60β1 subunits likely initiate oligomerization. While CPN60β protomers and homo-oligomers possessed ATPase activity, only the CPN60αβ1β2 oligomeric complex showed functional cooperation with GroES in refolding a model substrate. The presence of both CPN60α and CPN60β, but not the individual subunit alone, could complement endogenous GroEL function *in vivo*, and GroEL obligate substrates were specifically recognized by CPN60 subunits. The stoichiometry of subunits in functional CPN60αβ1β2 was determined. Down-regulation of the CPN60α subunit in *Chlamydomonas* resulted in a slow growth defect and an inability to grow autotrophically.

RESULTS

Chloroplast Chaperonin CPN60 Is Composed of Three Subunits

The *Chlamydomonas reinhardtii* genome encodes three chloroplast targeted chaperonin genes, *CPN60α*, *CPN60β1*, and *CPN60β2*, and three chaperonin co-factor genes, *CPN11*, *CPN20*, and *CPN23*. To understand whether and how these proteins form the CPN60 chaperonin complex *in vivo*, we first examined their oligomeric states in cells. Soluble *Chlamydomonas* extracts in the presence and absence of nucleotides were separated by native gel and visualized by immunoblotting with the CPN60 antibody. The majority of CPN60 formed oligomers with a mass of about 800 kDa, and only a minor portion of CPN60 formed monomers (Figure 1A). This distribution was unaffected by the presence of ATP/Mg or ADP/Mg (Figure 1A). Monomers containing CPN60 were detectable but largely degraded into

Band	Protein name	Peptides	Coverage (%)	Localization	Sc	Sc ratio
A1	CrCPN60c	37	74.67	Mitochondria	663	0.41
	CrCPN60α	23	53.79	Chloroplast	430	0.27
	CrCPN60β2	7	31.37	Chloroplast	142	0.09
	CrCPN60β1	6	16.90	Chloroplast	89	0.06
A2	CrCPN60α	30	50.86	Chloroplast	537	0.37
	CrCPN60β2	15	39.34	Chloroplast	282	0.19
	CrCPN60β1	8	20.69	Chloroplast	162	0.11
	CrCPN60c	4	11.92	Mitochondria	43	0.03
A3	CrCPN60α	103	81.90	Chloroplast	2299	0.40
	CrCPN60β2	96	84.75	Chloroplast	1909	0.34
	CrCPN60β1	56	72.76	Chloroplast	1286	0.23

Table 1. Summary of the Chaperonin Peptides Detected in the Gel Slices.

smaller fragments less than 60 kDa upon SDS–PAGE in the second dimension (Figure 1B, bottom panel). A signal in the 550-kDa region in the native PAGE represented large quantities of native Rubisco holoenzyme complex (Figure 1A and Supplemental Figure 1), and SDS–PAGE in the second dimension clearly showed that some CPN60 co-migrated with native Rubisco (Figure 1B, bottom panel), suggesting that CPN60 subunits may assist in assembly of Rubisco holoenzyme or comigration was an artifact due to the large quantity of Rubisco produced in chloroplast.

To elucidate the composition of CPN60 complexes *in vivo*, CPN60 complexes from cell lysates were immunoprecipitated with antiserum against CPN60α, or the CPN60 co-factor, CPN20, which was shown to interact with CPN60 *in vivo* in both *Arabidopsis* (Koumoto et al., 1999). Complexes were then eluted by competition with excess recombinant monomeric CPN60α protomer ($CPN60\alpha_{-M}$) or CPN20 and analyzed by 6% native PAGE followed by silver staining. As shown in Figure 1C, complexes precipitated with the CPN60α antibody migrated as two distinct bands (designated A1 and A2), whereas complexes precipitated with the CPN20 antibody migrated as a single band (designated A3), which corresponded to the lower band of the former. These three bands were carefully excised and analyzed by liquid chromatography-tandem mass spectrometry (LC-MS/MS) using a TripleTOF 5600 mass spectrometer (AB SCIEX, Vaughn, ON, Canada) coupled to an Eksigent NanoLC (Eksigent, Dublin, CA). The vast majority of the peptides detected from the three bands were derived from the chloroplast CPN60 subunits, CPN60α1, CPN60β1, and CPN60β2 (summarized in Table 1). The A1 and A2 bands also contained CPN60c, a CPN60 subunit localized in the mitochondria. However, sequence coverage and the spectrum counts (Sc) ratios (the ratio of the peptide of interest in the total peptides detected), indicate that CPN60c was more dominant in the A1 band and chloroplast-localized CPN60 subunits were more dominant in the A2 band (Table 1). It is probable that CPN60c oligomers were immunoprecipitated because the CPN60α antibody, which has low specificity, recognizes both CPN60α and CPN60c. Precipitation with the CPN20 antibody, however, yielded only one unique band (Figure 1C), and importantly, only the three chloroplast CPN60 subunits were detected by mass spectrometry (MS) with combined Sc ratios of up to 97% (Table 1). These data are consistent with the notion that CPN20 interacts with chloroplast CPN60 complexes but not with mitochondrial CPN60c oligomers.

Three CPN60 Oligomeric Complexes without a Flexible C-Terminal Tail Identified *In Vitro*

To determine whether the chloroplast CPN60 oligomers were composed of a homogeneous population of oligomers with distinct subunits or a heterogeneous population of oligomer types, oligomer formation was assessed after expression of recombinant CPN60 genes in the *E. coli* cellular environment. Co-expressed genes shared the same T7 promotor and terminator for co-transcription but had their own ribosomal binding sites, start codons, and stop codons for translation (Supplemental Figure 2A). The co-expression of these proteins was confirmed by MS, and induced protein amounts and protein solubility were also visualized by SDS–PAGE upon fractionation of cell extracts (Supplemental Figure 2B). In all constructs, expression of *CPN60* genes from isopropyl β-D-1-thiogalactopyranoside (IPTG)-induced plasmids resulted in similar amounts of soluble CPN60 protein, irrespective of whether the CPN60 genes were expressed individually or in combination (Supplemental Figure 2B). The formation of CPN60 oligomers was then monitored by native PAGE followed by Coomassie staining (Figure 2A). Consistent with published results (Dickson et al., 2000), CPN60α alone did not form oligomers, while a significant portion of CPN60β1 and CPN60β2 assembled into oligomers (Figure 2A). Surprisingly, CPN60 oligomer formation of either CPN60β1 or CPN60β2 was dramatically reduced in the presence of CPN60α (Figure 2A, CPN60αβ1 and CPN60αβ2), suggesting that CPN60α disturbs the assembly of the CPN60β homo-oligomer. Importantly, CPN60 oligomer formation recovered upon co-expression of three protomers (Figure 2A, CPN60αβ1β2), indicating that CPN60 oligomer formation is promoted by the presence of all three CPN60 subunits in the cellular environment.

The three types of CPN60 oligomers, CPN60β1, CPN60β2, and CPN60αβ1β2, were purified using chromatography (Figure 3A and Supplemental Figure 2C), and the purity and composition of the oligomers were confirmed by MS, ruling out contamination by endogenous GroEL. Purification of oligomers

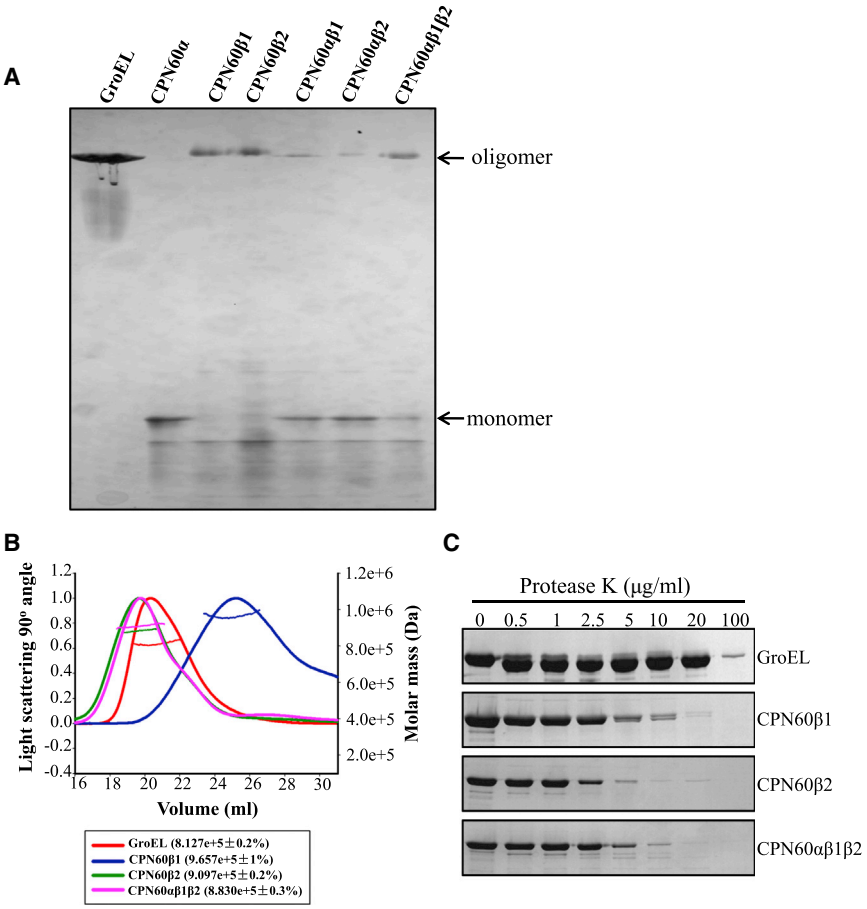

Figure 2. Formation of CPN60 Oligomers upon Expression in *E. coli*.

(A) CPN60 oligomer formation from induced CPN60 subunits. CPN60 subunits were expressed individually or in combination, and soluble fractions were visualized by colorless 5%–13% gradient native PAGE and staining with Coomassie brilliant blue.

(B) Mass determination of recombinant purified oligomers by AFFFF–MALS. Calculated values for the molar mass of purified proteins are shown on the *y* axis and in the lower text box. Horizontal lines across the peaks indicate the molar mass and homogeneity of the sample.

(C) The 0.5 μg/μl chaperonin complexes were incubated with proteinase K for 30 min at 25°C and proteolysis was stopped with 1 mM phenylmethylsulfonyl fluoride. The digested chaperonin was visualized after Coomassie staining of 10% SDS–PAGE gels.

of CPN60αβ1 and CPN60αβ2 was not possible because these oligomers did not accumulate in sufficient amounts (Figure 2A). Oligomers of CPN60β1, CPN60β2, and CPN60αβ1β2 migrated at different positions in a 6% native PAGE (Supplemental Figure 2C), suggesting that the oligomers were homogeneous rather than heterogeneous in composition. For molecular weight analysis, the oligomers were subjected to asymmetrical field flow fractionation (AFFFF) followed by multiple-angle light scattering (MALS) (Figure 2B). The three types of CPN60 oligomers were 880–960 kDa in size and composed of 14–16 subunits (Figure 2B). Considering the symmetric double-ring structures of GroEL and TriC/CCT, as well as the more precise measurement of the molecular weight of purified recombinant *Arabidopsis* CPN60$\alpha_7\beta_7$ (Tsai et al., 2012), the chloroplast chaperonin oligomers are likely tetradecamers.

The C-terminus of GroEL subunits protrudes from the equatorial domain and it was sensitive to proteinase K (PK); 16 amino acids were removed by PK as expected (Hayer-Hartl et al., 1995) (Figure 2C and Supplemental Figure 2D). However, PK treatment of CPN60β1, CPN60β2, and CPN60αβ1β2 oligomers did not liberate a PK-resistant fragment in a similar manner (Figure 2C), suggesting that CPN60 oligomers do not have flexible C-terminal tails like GroEL. Furthermore, CPN60β1, CPN60β2, and CPN60αβ1β2 oligomers were almost completely digested in the presence of 10 μg/ml protease, whereas GroEL was largely digested only with 100 μg/ml protease (Figure 2C). This result suggests that CPN60 oligomers are not as tightly compacted as those of GroEL, which may explain why the molecular weight of CPN60 oligomers appeared larger than that of GroEL as measured by AFFFF–MALS (Figure 2B).

The Dynamic Nature of CPN60 Oligomers Is Mediated by Subunit Composition and ATP

The refolding ability of the homo-oligomer CPN60β has been characterized *in vitro* (Vitlin et al., 2011) but the stability of homo-oligomer in the presence of nucleotides and other protomers has not yet been reported. We therefore analyzed the effect of nucleotides and protomers on the CPN60 oligomers identified herein. We first analyzed their oligomeric states in the presence of nucleotides using native PAGE and Coomassie staining (Figure 3A). Under control conditions, ATP slightly stimulated the formation of single-ring GroEL (SR-GroEL) (Figure 3A, lane 5). The GroEL-SR produced by ATP hydrolysis, little reported previously, might result from the electrophoresis conditions here. CPN60 oligomers were differentially affected by ATP, with ATP causing no observable effect on CPN60β1 oligomers (Figure 3A, lane 6), complete disassembly of CPN60β2 oligomers (Figure 3A, lane 7), and marginally enhanced disassembly of CPN60αβ1β2 oligomers (Figure 3A, lane 8) into monomers. The addition of ADP also stimulated the formation of single-ring GroEL (Figure 3A, lane 9) but had no effect on the three types of CPN60 oligomers (Figure 3A, lanes 10–12). Sequence alignment showed that the ATP-binding sites on the CPN60β1 and CPN60β2 subunits are conserved (Supplemental Figure 3), suggesting that ATP binding should not account for their differing disassembly behavior. In addition, CPN60β2 did not disassemble into monomers in the presence of the non-hydrolysable ATP analogue AMP-PNP (Supplemental Figure 4A), indicating that disassembly of homo-oligomers of CPN60β2 requires ATP hydrolysis.

To further investigate the disassembly time course of CPN60β2, ATP was converted to ADP by hexokinase/glucose at different

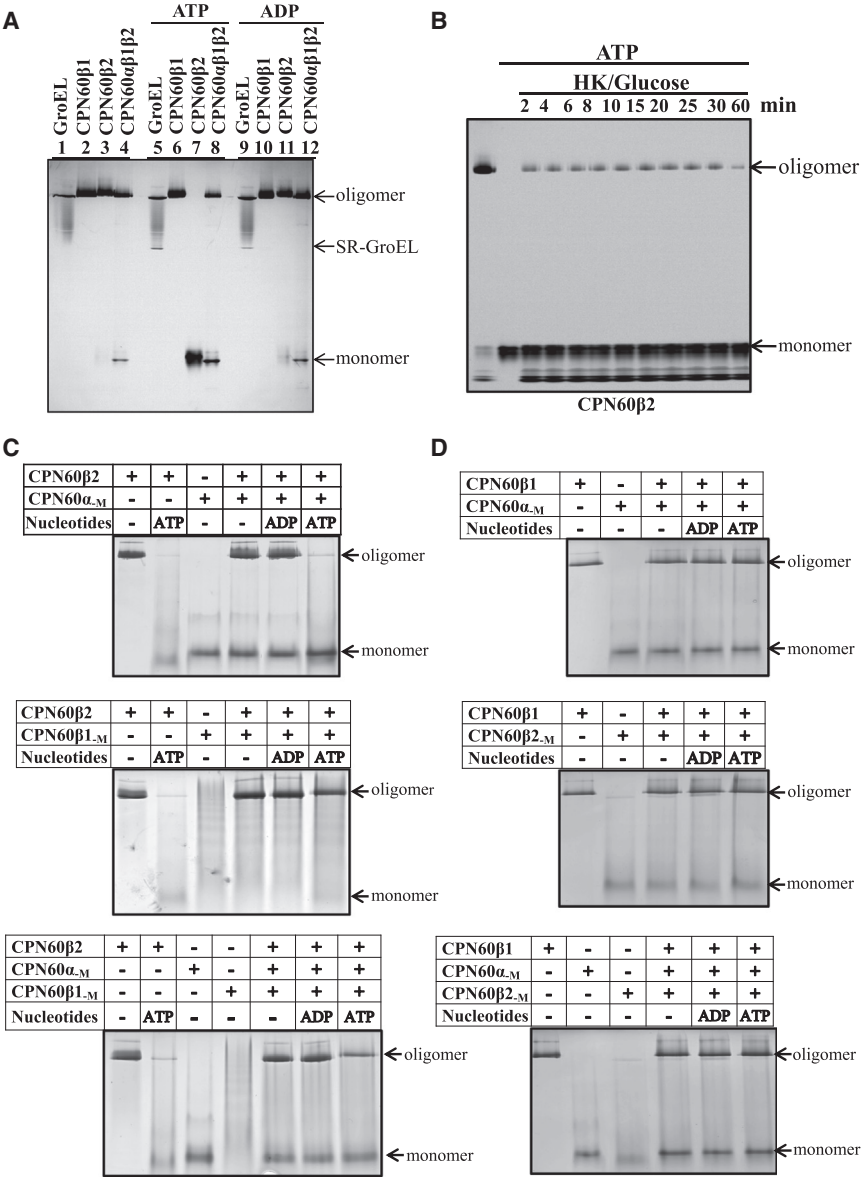

Figure 3. Oligomeric States and Composition of CPN60 Chaperonin.

(A) Oligomeric states of purified CPN60 oligomers in the presence of nucleotides. In total, 0.5 mg/ml chaperonin oligomers were incubated with ATP/Mg (5 mM) or ADP/Mg (5 mM) for 30 min at room temperature, followed by separation with colorless 5%–13% gradient native PAGE and visualized by Coomassie brilliant blue staining.

(B) Oligomeric states of CPN60β2 complexes. 0.5 mg/ml CPN60β2 oligomers were incubated with 5 mM ATP/Mg and ATP was depleted upon addition of hexokinase (HK)/glucose at the indicated time points. The mixtures were separated with colorless 5%–13% gradient native PAGE and visualized by Coomassie brilliant blue staining.

(C and D) Composition of CPN60 oligomers in the presence of other protomers and nucleotides. 0.2 mg/ml homo-oligomeric CPN60β2 **(C)** and homo-oligomeric CPN60β1 **(D)** were incubated with 0.2 mg/ml of one protomer or the other two protomers (0.1 mg/ml each), and/or 2 mM nucleotides as indicated for 30 min at 25°C. Samples were then loaded on a 6% mini-native PAGE gel and visualized by Coomassie brilliant blue staining.

incubation times, and the oligomeric states of CPN60β2 were visualized by native PAGE and Coomassie staining (Figure 3B). The majority of the oligomers disassembled into monomers within 2 min but minor amounts were detected in the oligomeric state even after incubation for 1 h (Figure 3B) and 5 h (Supplemental Figure 4B). The same results were observed upon addition of apyrase to convert ATP into AMP (Supplemental Figure 4C). These results indicate that disassembly of CPN60β2 oligomers in the presence of ATP occurs rapidly (in less than 2 min). The presence of a minor amount of oligomers of CPN60β2 upon ATP depletion could reflect the conversion of assembly-capable monomers back into oligomers.

The three Cpn60 protomers (CPN60α_{-M}, CPN60$\beta1_{-M}$, and CPN60$\beta2_{-M}$) were recombinantly purified, while CPN60$\beta1_{-M}$ subunits were purified as a mixture of multiple oligomeric forms smaller than tetradecamers (Figure 4A, lane 3). We further investigated the stability of homo-oligomers in the presence of other purified protomers and nucleotides. Nucleotides and CPN60 protomers were incubated with either of the CPN60β homo-oligomers (Figure 3C and 3D). In the presence of ATP, oligomeric CPN60β2 again disassembled into monomers (Figure 3A and 3C), with small amounts of oligomer detected upon addition of CPN60α_{-M} (Figure 3C, top gel, rightmost lane), which was detected in the oligomers by MS with Sc ratios of 33% (Supplemental Table 1, band CPN60β2 + CPN60α_{-M}). Upon addition of CPN60$\beta1_{-M}$, the amount of oligomers increased dramatically and oligomer mobility was shifted slightly in the presence of ATP (Figure 3C, middle gel, rightmost lane). Simultaneously, CPN60β1 was detected in the oligomers by MS with unique peptide Sc ratios of 43% (Supplemental Table 1, band CPN60β2 + CPN60$\beta1_{-M}$). Similarly, in the presence of ATP and the other two subunits, a substantial amount of oligomers was detected and complex mobility was slightly altered (Figure 3C, bottom gel, rightmost lane), with CPN60α subunits with Sc ratios of 12% as well as CPN60β1 subunits with Sc ratios of 36% detected in the oligomers (Supplemental Table 1, band CPN60β2 + CPN60α_{-M} + CPN60$\beta1_{-M}$). In addition, in the presence of ADP or in the absence of nucleotides, homo-oligomeric CPN60β2 was very stable and the mobility was not affected by the addition of the other two protomers (Figure 3C). These results emphasize that homo-oligomeric CPN60β2 is highly unstable in the presence of ATP but readily forms a stable oligomeric complex with either or both CPN60 protomers that is protected from complete dissociation into monomers in the presence of ATP.

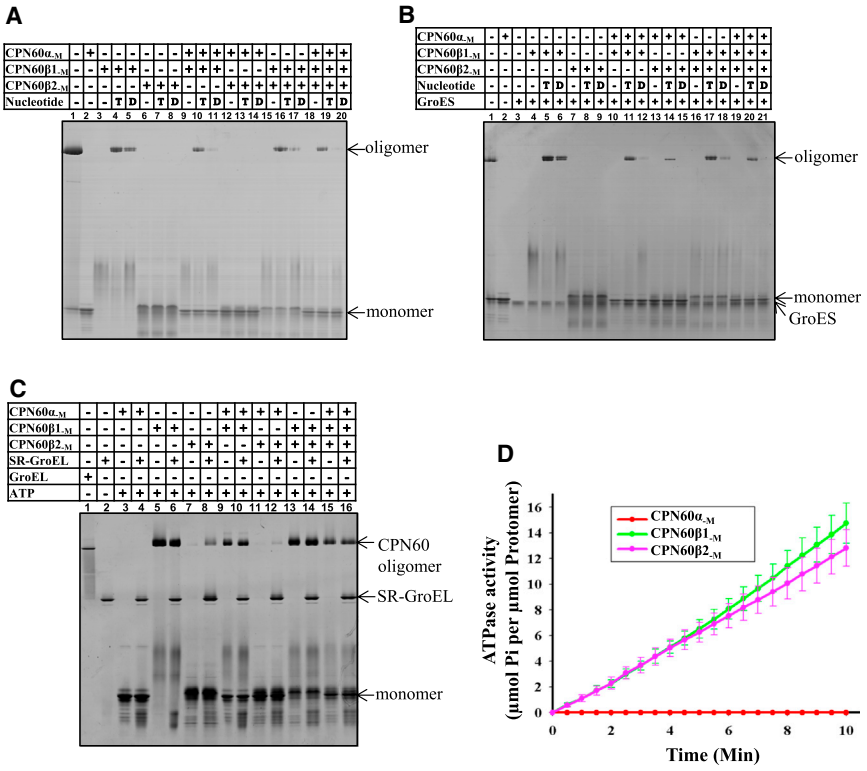

Figure 4. Contribution of CPN60 Protomers and Other Factors on Oligomer Assembly and ATPase Activity.

(A) 0.45 mg/ml chaperonin protomers (when two or three protomer types were used, each type was present in equal amounts) were incubated with or without 4 mM nucleotides (T stands for ATP, D stands for ADP) for 5 min at room temperature and then for 1 h at 30°C. Samples were then loaded on a 5%–13% gradient colorless native PAGE gel and visualized by Coomassie staining. Cpn60αβ1β2 was loaded in lane 1 as control.

(B) 0.45 mg/ml chaperonin protomers (when two or three protomer types were used, each type was present in equal amounts) were incubated with or without 4 mM nucleotides (T stands for ATP, D stands for ADP), and with or without 0.25 mg/ml co-chaperonin GroES, for 5 min at room temperature and then for 1 h at 30°C. Samples were then loaded on a 5%–13% gradient colorless native PAGE gel and visualized by Coomassie staining.

(C) 0.45 mg/ml chaperonin protomer (when two or three protomer types were used, each type was present in equal amounts) were incubated with 4 mM ATP in buffer (20 mM MOPS/KOH [pH 7.5], 100 mM KCl, 5 mM $MgCl_2$, 2 mM DTT) in the absence or presence of 0.2 mg/ml GroEL-SR for 5 min at room temperature and then for 1 h at 30°C. Samples were then loaded on 5%–13% gradient colorless native PAGE and visualized by Coomassie staining.

(D) ATPase activity of CPN60 protomers. The ATPase rate of 2.8 μM CPN60 protomers (equal to 0.2 μM oligomer) was measured for 10 min at 25°C.

In contrast, homo-oligomeric CPN60β1 was highly stable in the presence of ATP (Figure 3A and Figure 3D) and the mobility of CPN60 oligomers was not affected in the presence of other protomers (Figure 3D). However, in the presence of ATP, added protomers were detected by MS with low Sc ratios (1%–6%) (Supplemental Table 1, bottom three rows), indicating that the added protomers may non-specifically associate with homo-oligomeric CPN60β1.

Reconstitution of CPN60 Oligomers in the Presence of Nucleotides and Co-chaperonin *In Vitro*

To examine chaperonin complex oligomerization and its requirements, we reconstituted oligomers using purified protomers *in vitro* and visualized reaction products using Coomassie staining of native PAGE. Considerable amounts of CPN60β1$_{-M}$ assembled into oligomers in the presence of ATP/Mg (Figure 4A, lane 4), while less oligomers were detected in the presence of ADP/Mg (Figure 4A, lane 5). On the other hand, CPN60β2$_{-M}$ remained monomeric regardless of the presence of ATP/Mg or ADP/Mg (Figure 4A, lanes 6–8). Oligomers containing CPN60β1$_{-M}$ were somewhat less abundant in the additional presence of CPN60α$_{-M}$ or CPN60β2$_{-M}$ and ATP (Figure 4A, lanes 4, 10 and 16), and these oligomers were dramatically reduced in the presence of ADP (Figure 4A, lanes 5, 11, and 17). This indicated that CPN60α$_{-M}$ and/or CPN60β2$_{-M}$ may have high affinity for CPN60β1$_{-M}$, which disturbs homo-oligomer assembly of CPN60β1$_{-M}$ alone. CPN60 oligomers were not detected in the presence of CPN60α$_{-M}$ and CPN60β2$_{-M}$ (Figure 4A, lanes 12–14); however, the presence of all three protomers readily promoted oligomer formation in the presence of ATP/Mg (Figure 4A, lane 19) and this effect was largely abolished in the presence of ADP/Mg (Figure 4A, lane 20). These results describing oligomer reconstitution *in vitro* are largely consistent with those describing oligomer formation upon recombinant co-expression in *E. coli*, except those concerning the homo-oligomer of CPN60β2 (Figure 4A and Figure 2A). The lack of homo-oligomeric CPN60β2 upon reconstitution *in vitro* may have been caused by missing cellular factors (e.g. chaperones) and/or ATP-mediated disassembly of newly formed oligomers (see Discussion). Overall, CPN60 complex formation from protomers *in vitro* depended on the presence of ATP and the critical presence of the CPN60β1$_{-M}$ protomer.

Chaperonin cofactors have been reported to potentiate the assembly of chaperonin oligomers *in vitro* but the natural co-factor of CPN60 in chloroplast remains unclear. Although CPN20 is a candidate co-factor, recombinantly expressed *Chlamydomonas* CPN20 does not functionally interact with GroEL and CPN60αβ *in vitro* (Tsai et al., 2012). We instead examined the influence of the GroEL co-factor GroES, which showed cooperation with CPN60 both *in vivo* and *in vitro* (Figure 5 and Figure 6) on CPN60 oligomer formation. Hetero-oligomer formation of CPN60α$_{-M}$/CPN60β2$_{-M}$ was indeed stimulated by the addition of GroES to the reaction (Figure 4B, lane 14; Figure 4A, lane 13) but the potentiation effect of GroES on the assembly of other CPN60 oligomers was not detected. The reconstituted oligomers (Figure 4B, lanes 11, 14, 17, and 20) contained the added CPN60 monomer subunits but none consisted of GroES, as detected by MS. We next analyzed the effect of the

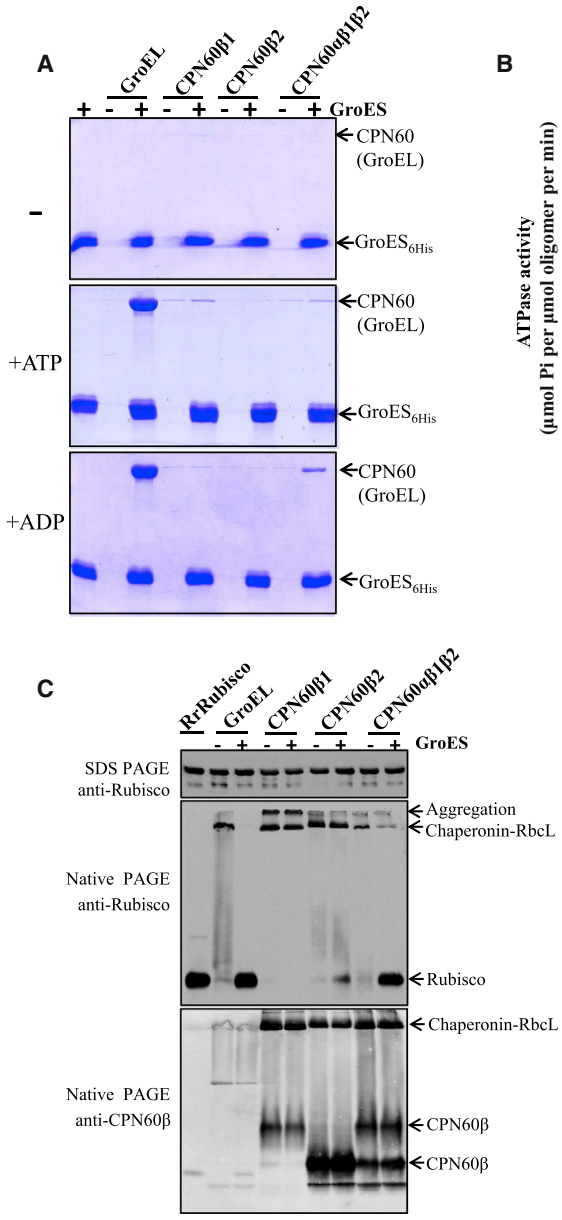

Figure 5. Cooperation of the Chaperonin and Co-factor GroES.

(A) Pull-down of chaperonin by co-chaperonin GroES. A total of 100 μg of $GroES_{6His}$ was immobilized on Ni-NTA beads and incubated with 50 μg of GroEL or CPN60 oligomers for 4 h at 25°C, and then supplied with 1 mM ATP or ADP. Proteins were eluted with 1 M imidazole after washing and resolved by 15% denaturing SDS–PAGE and visualized by Coomassie staining.

(B) ATPase assays of chaperonin in the presence or absence of co-chaperonin GroES. The ATPase rate of GroEL or CPN60 oligomers (0.2 μM oligomer each) was measured in the absence or presence of co-chaperonin GroES (0.5 μM oligomer) at 25°C.

(C) Refolding capability of CPN60 oligomers. A total of 50 μM chemically denatured Rubisco was diluted 100-fold into buffer containing 1 μM chaperonin oligomers. The supernatant was supplied with 1 mg/ml bovine serum albumin and 1 μM co-chaperonin; the refolding was initiated by adding 2 mM ATP for 1 h at 25°C and stopped with 10 mM glucose and 2.5 U of hexokinase. The reaction samples were separated either by SDS–PAGE or 5%–15% colorless native PAGE and immunodetected using anti-Rubisco serum and anti-CPN60 serum.

heptameric single-ring variant of GroEL and the tetradecameric GroEL on oligomerization of protomers. As shown in Figure 4C, SR-GroEL potentiated the assembly of homo-oligomeric CPN60β2 (Figure 4C, lane 8) and hetero-oligomeric CPN60αβ2 (Figure 4C, lane 12). However, GroEL in its double-ring form had no effect on the assembly of CPN60 oligomers (Supplemental Figure 5). The stimulatory effect of GroES and SR-GroEL was only observed in the assembly of a subset of CPN60 oligomers, all of which contain the $CPN60\beta2_{-M}$ protomer but not the $CPN60\beta1_{-M}$ protomer, which is already assembly prone on its own. These results indicate that GroES or SR-GroEL might function as a template to provide the scaffold for CPN60β2 assembly.

Since ATP was indispensable for oligomer assembly, we also assessed ATP hydrolysis of purified protomers (Figure 4D). $Cpn60\alpha_{-M}$ had no ATPase activity, while both $Cpn60\beta2_{-M}$ and $Cpn60\beta1_{-M}$ possessed high ATPase activity (Figure 4D), even though only Cpn60β1 (but not Cpn60β2) formed substantial homo-oligomers (Figure 4). These results suggested that oligomer assembly may not consume ATP but, instead, ATP hydrolysis may induce a conformational change in the monomer that makes it competent for assembly.

Cooperation between CPN60 and Co-chaperonin GroES

We next investigated the interaction of CPN60 complexes with co-chaperonin GroES *in vitro* with recombinantly purified proteins. We pulled down chaperonin oligomers using GroES with a C-terminal His6-tag ($GroES_{6His}$) by immobilized metal affinity chromatography. As shown in Figure 5A, no chaperonin oligomers were pulled down in the absence of nucleotides (top panel). In the presence of ATP, high concentrations of GroEL were pulled down, as expected, and very small amounts of CPN60β1 and CPN60αβ1β2 oligomers were also pulled down (Figure 5A, middle panel). In the presence of ADP, a substantial amount of CPN60αβ1β2 was pulled down, although much less than GroEL (Figure 5A, bottom panel). These results indicate that the presence of ADP dramatically enhances the interaction of pre-formed oligomers of CPN60αβ1β2 with GroES. We next performed the ATPase assay to investigate the ATPase activities of three isolated CPN60 oligomers in the presence or absence of GroES. CPN60β1, CPN60β2, and CPN60αβ1β2 possessed higher ATPase activity than GroEL (Figure 5B). GroES did not inhibit the ATPase activity of CPN60β1 or CPN60β2 oligomers.

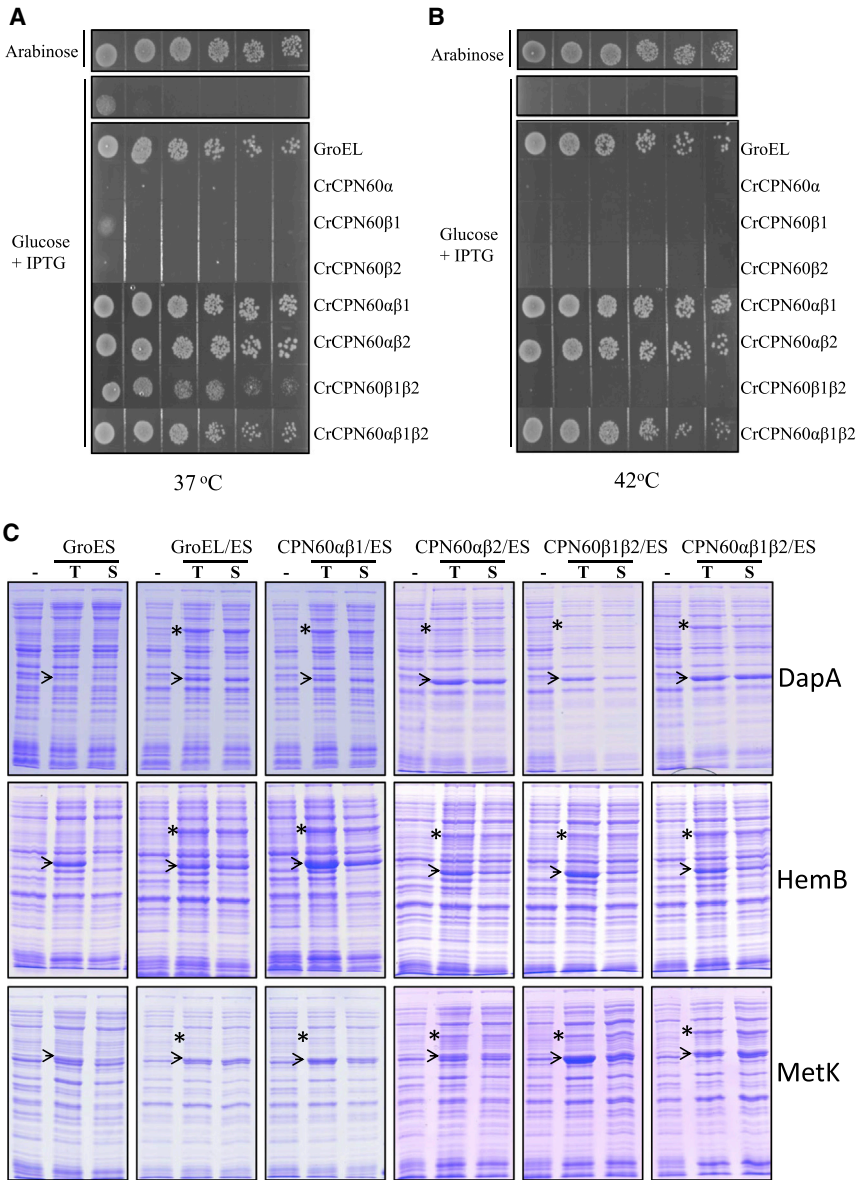

Figure 6. Functional Replacement of GroEL by CPN60.

(A and B) CPN60s complement GroEL function. *E. coli* strain MGM100, in which endogenous *groE* promotor is replaced by pBAD promotor, was transformed with plasmids containing isopropyl β-D-1-thiogalactopyranoside (IPTG)-inducible *GroES-GroEL*, *GroES-CPN60α*, *GroES-CPN60β1*, *GroES-CPN60β2*, *GroES-CPN60αβ1*, *GroES-CPN60αβ2*, *GroES-CPN60β1β2*, *GroES-CPN60αβ1β2*, and grown on medium supplemented with glucose and IPTG at 37°C **(A)** or 42°C **(B)** for 15 h.

(C) Folding of GroEL obligate substrates by CPN60. Three GroEL obligate substrates were induced for 3 h in MGM100 cells in which GroES, GroEL/ES, CPN60αβ1/GroES, CPN60αβ2/GroES, CPN60β1β2/GroES, or CPN60αβ1β2/GroES was overexpressed. The solubility of the substrates was then analyzed by SDS–PAGE. For each panel, total lysate from uninduced cells (-), total lysate from induced cells (T), and the soluble fraction (S) of induced-cell lysate were loaded in the indicated lanes. The induced chaperonin and substrates are indicated with * and an arrowhead, respectively.

However, CPN60αβ1β2 showed about 50% decreased ATPase activity in the presence of GroES, similar to the inhibition effect on GroEL (Figure 5B). These results suggest a functional interaction between CPN60αβ1β2 and the co-chaperonin GroES *in vitro*.

The substrate refolding capacity of CPN60 oligomers was further investigated. Denatured Rubisco captured by chaperonin oligomers was refolded in the absence or presence of co-chaperonin GroES for 1 h. The samples were separated on 5%–15% colorless native PAGE and visualized by immunoblotting with serum against either Rubisco or CPN60. As shown in Figure 5C, the amount of Rubisco in the supernatant was comparable (top panel), while oligomers displayed different Rubisco refolding capabilities (middle native PAGE). Homo-oligomeric CPN60β1 displayed no refolding ability, while CPN60β2 showed very little refolding capability regardless of the presence of co-chaperonin GroES. After the reaction was stopped and stored for 3 days at 4°C, the amount of Rubisco released from chaperonin increased significantly independent of the presence of GroES (Supplemental Figure 6). Similar to GroEL, the refolding capability of CPN60αβ1β2 was dependent on the co-chaperonin GroES.

Functional Complementation of GroEL by CPN60

We next investigated if individual or a combination of CPN60 subunits could complement GroEL function *in vivo*. In the *E. coli* MGM100 strain (MG1655 groE::araC-PBAD-groE [Kan^r], *E. coli* Genetic Stock Center, Yale) (McLennan and Masters, 1998), the promoter of the groE operon is replaced with the tightly regulated pBAD promoter, resulting in expression of the endogenous GroEL/ES operon in the presence of arabinose but not in the presence of glucose, a condition lethal to the cells. To study complementation of GroEL function by individual or a combination of CPN60 subunits, MGM100 was transformed with the pOFX-GroE plasmid in which GroES and GroEL are under an IPTG-inducible Lac promoter and operator (Castanie et al., 1997) or pOFX-CPN60 plasmids containing GroES together with individual or a combination of *CPN60* genes from *Chlamydomonas*. As shown in Figure 6A, the expression of individual subunits of CPN60 with GroES could not complement GroEL/ES function *in vivo* in the presence of glucose and IPTG, in contrast to induced expression of GroEL/ES. However, co-expression of two or three CPN60 subunits with GroES permitted cell growth but in cells expressing the combination of CPN60β1 and CPN60β2 with GroES, an observable growth defect persisted (Figure 6A), and this specific combination could no

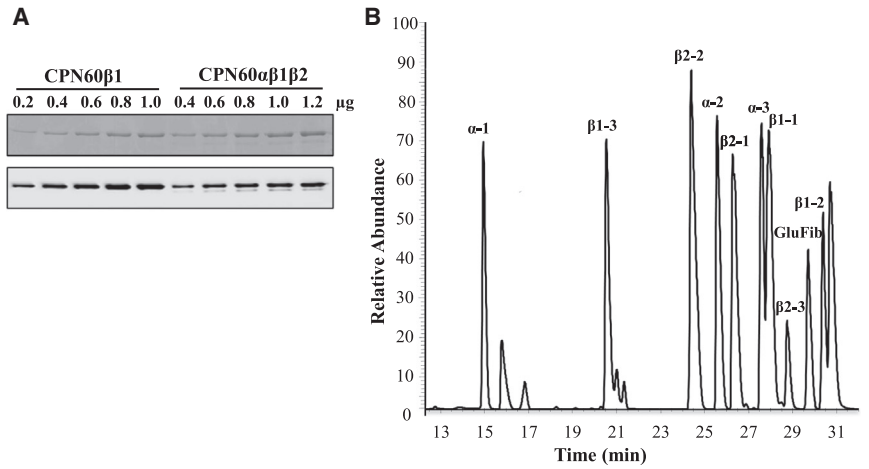

Figure 7. Stoichiometry of Three CPN60 Subunits within Tetradecamer.

(A) Representative immunoblot for determination of stoichiometry. Purified proteins with indicated amounts were separated using SDS–PAGE and analyzed by immunoblotting. The relative signal density was quantified with Quantity One (Bio-Rad) for five independent experiments.

(B) Extracted ion chromatograms of the selected proteolytic peptides. The abundance and retention time of heavy isotope-labeled peptides derived from CPN60-QconCAT proteins are shown.

longer complement GroEL/ES function when cells were subjected to heat shock at 42°C (Figure 6B). These results suggest that the presence of both CPN60α and CPN60β subunits was required with co-factor GroES to assist in the folding of all GroEL substrates essential for normal growth.

Since CPN60 could complement GroEL function *in vivo*, three GroEL obligate substrates, DapA, HemB, and MetK (Kerner et al., 2005; Fujiwara et al., 2010), were used to study whether CPN60 subunits recognize substrates specifically. The substrate proteins were induced in the MGM100 cells in which either GroEL/ES or CPN60/GroES are overexpressed as described above. The solubility of substrate proteins was monitored by SDS–PAGE followed by Coomassie staining. DapA was found to be insoluble in cells overexpressing CPN60β1β2 but stayed soluble in cells expressing CPN60 combining with CPN60α subunits (Figure 6C, top panel). This result indicated that the CPN60α subunit was indispensable to folding of DapA. HemB protein was completely soluble in cells expressing GroEL but was largely insoluble in cells expressing with CPN60s (Figure 6C, middle panel). Whereas only CPN60αβ1β2 was similar to GroEL in its ability to fold substrate MetK, other combinations of CPN60 subunits partially promoted MetK solubility. These results indicated that the folding capacity of CPN60 subunit combinations in folding GroEL obligate substrates varies significantly and GroEL substrates are specifically recognized by certain CPN60 subunits.

Stoichiometry of Three CPN60 Subunits in the Tetradecamer

It has been proposed that chloroplast CPN60 is composed of seven α and seven β types of subunits. We analyzed the stoichiometry of each subunit within recombinantly purified CPN60αβ1β2 with immunoblot and absolute MS quantification. We developed peptide antibodies recognizing CPN60β1 subunits specifically. Different amounts of CPN60β1 and CPN60αβ1β2 were loaded on the SDS–PAGE and the immunoblot signal was compared using Quantity One software (Bio-Rad) (Figure 7A). The signal intensity corresponding to the loaded protein in varying amount was linearized with high precision (Supplemental Figure 7). CPN60β1 was 39.11 ± 5.73% in the CPN60αβ1β2 tetradecamer which accounts for 5.48 ± 0.80 CPN60β1 subunits.

We also implemented the QconCAT approach to determine the molar ratio of each subunit in the oligomers (Pratt et al., 2006; Olinares et al., 2011). We first synthesized one gene (designated *CPN60-QconCAT*) encoding a total of nine CPN60 subunit-derived peptides (Table 2) and two additional peptides as controls. The gene was constructed in a vector containing a C-terminal His6 tag for affinity purification and expressed in *E. coli* cells grown in minimal medium containing [$^{13}C_6$]-Lys and [$^{13}C_6$]-Arg to label CPN60-QconCAT protein with isotope. Purified CPN60-QconCAT or CPN60αβ1β2 protein was digested with trypsin and assessed by mass spectrometer Q Exactive (Thermo Scientific) equipped with an Easy-nLC 1000 HPLC system (Thermo Scientific). The derived heavy isotope-labeled CPN60 peptides were separated with high precision (Figure 7B). The peak areas of each peptide corresponding to extracted ion chromatograms (XIC) were assessed and L/H ratios were calculated for two independent experiments (Table 3). The resulting stoichiometry for CPN60α, CPN60β1, CPN60β2 was 5, 6, 3, respectively, in tetradecamer, which is consistent with the immunoblot results (Figure 7A).

Down-Regulation of CPN60α in *Chlamydomonas*

Since the CPN60α subunit is indispensable for complementing GroEL function in *E. coli* (Figure 6A) and the insertion mutant of the Cpn60α subunit is lethal to plants (Barkan, 1993; Suzuki et al., 2009), we next investigated the effect of down-regulation of the *CPN60α* gene on *Chlamydomonas* cells. We used artificial miRNA (amiRNA) to reduce *CPN60α* expression. *Chlamydomonas* endogenous miRNA MIR1157 was combined with the 3′ UTR region of *CPN60α* (TCTGTTTAGATGGTC ATCCCG) by a multi-annealing method described by Hu et al. (2014). The fragment was then ligated into plasmid pHK85 for *CPN60α*-amiRNA construction, in which expression of amiRNA is driven by the *PSAD* promoter and the *AphVIII* gene (paromomycin resistance) was used as a selective marker for transformants. The construct silenced the *CPN60α* gene efficiently, as shown by the reduction in the *CPN60α* mRNA level to <10% of wild-type levels from three representative lines (Figure 8A). And CPN60α-amiRNA cells showed retarded growth at moderate light intensities (45 μmol photons m^{-2} s^{-1}) in Tris-acetate-phosphate (TAP) medium (Figure 8B). Strain 14 was identified 3 months earlier than the other two strains, and the growth defect lessened with time; this may occur when the amiRNAi construct itself is silenced over time as has been reported (Nordhues et al., 2012). The amiRNA strains grew

Subunits	Peptide	Sequence	*m/z*	MS[a]
CPN60α	α-1	ETLTDAEEK	518.2468 (+2)	Y
	α-2	VADAVGVTLGPR	577.8312 (+2)	Y
	α-3	VEQAVVEQLGVAR	699.3921 (+2)	Y
CPN60β1	β1-1	IVSAGTNPVQLVR	677.3977 (+2)	Y
	β1-2	GYTSPYFVTDPER	766.3582 (+2)	N
	β1-3	TTVVGDGSTAADVAAR	745.8776 (+2)	Y
CPN60β2	β2-1	ATEEVLGLAAK	551.3117 (+2)	Y
	β2-2	IVAAGTNPVQLTR	670.3898 (+2)	Y
	β2-3	DELGITLEK	745.8776 (+2)	N

Table 2. Selected CPN60 Peptides from Three Subunits for Absolute Quantification.
[a]The peptides were detected by MS but not used in the analysis because the MS peak area overlapped with other peptides.

better at low light intensity (15 μmol photons m^{-2} s^{-1}) than in moderate light conditions (Figure 8C) but they could not survive on minimal medium in which the carbon source is absent and therefore cells must grow autotrophically (Figure 8D). These results suggest that autotrophic growth is impaired in *CPN60α*-amiRNA strains. Moreover, the *CPN60α*-amiRNA strains could not grow after heat shock treatment (Figure 8E), suggesting that the function of the chaperonin system is deficient.

Western analyses of plant extract, with elongation factor-Tu (EF-Tu) as an internal control, revealed that the CPN60α protein level was not reduced in amiRNAi strains (Figure 8F), probably as a result of the cross-reactivity of the antiserum with all three CPN60 subunits. Chaperonin co-factor CPN20 and the potential substrate Rubisco large subunit (RbcL) were not reduced. In contrast, the expression level of chloroplast chaperone Hsp70 (HSP70B) and the nucleotide exchange factor (CGE1) of Hsp70 increased, suggesting that the Hsp70 system might partially compensate for reduced chaperonin function.

DISCUSSION

Dynamic Nature of CPN60 Oligomers Mediated by ATP

We detected oligomers containing CPN60 chaperonin subunits in chloroplast extracts from *Chlamydomonas* and upon heterologous expression in *E. coli* (Figure 1A and Figure 2A). Certain chaperonin oligomers that were synthesized in the *E. coli* cellular environment and then purified showed a dramatic sensitivity to ATP, disassembling completely upon exposure to ATP (Figure 3A, CPN60β2). This disassembly reaction required ATP hydrolysis for only 2 min (Figure 3B) and was greatly influenced by the additional presence of other CPN60 assembly partners (Figure 3C). The CPN60β2 oligomer, which was highly sensitive to ATP-induced disassembly, for instance, became more resistant to disassembly upon incorporation into CPN60β1β2 or CPN60αβ1β2 oligomers (Figure 3A and Figure 3C). Suppression of this effect by incorporation into, for example, the CPN60αβ1β2 complex may be due to a conformational change in the CPN60β2 oligomer that confers resistance to ATP-mediated disassembly.

ATP-mediated partial disassembly may be a phenomenon specific to chloroplast Cpn60 chaperonin as it has also been detected for Cpn60 in pea plants (Viitanen et al., 1995), but never for GroEL in *E. coli* or TriC/CCT in eukaryotic cytosol. It is therefore tempting to speculate that ATP-mediated disassembly of Cpn60 is integrally linked to its chloroplast-specific assembly or function. With this idea in mind, it may seem surprising that CPN60 chaperonin oligomers formed in *Chlamydomonas* chloroplast did not disassemble in cell lysate exposed to ATP (Figure 1A). However, assembled chaperonin oligomers from *Chlamydomonas* containing all three subunits (Figure 1C) should be largely protected from ATP-mediated disassembly (Figure 3A, lane 8).

CPN60 reconstitution *in vitro* was driven by ATP only in reactions containing the CPN60β1$_{-M}$ protomer (Figure 4A). The lack of stable oligomers detected in reactions containing ATP and CPN60β2$_{-M}$ (Figure 4A, lanes 7 and 13) may have been the result of rapid ATP-mediated disassembly of newly formed oligomers consistent with our previous results (Figure 3A). This effect was suppressed upon incorporation of CPN60β2$_{-M}$ into stable oligomers containing the other two subunits (Figure 4A, lane 19), as was predicted from our data from *E. coli* (Figure 3A and 3C). Our data suggest a dual role for ATP. First, ATP stimulates oligomerization of protomers. Second, ATP also mediates rapid disassembly, a process essential to chloroplast chaperonin function, of certain oligomers. Both of these effects could be caused by ATP-induced conformational changes that render the protomer/oligomer assembly competent or disassembly prone.

The biogenesis of chaperonin oligomers *in vivo* resulting from self-assembly and/or stimulation by unknown factors is a long-standing question. Lissin et al. (1990) reported that GroEL oligomers first formed spontaneously and then further assembly was stimulated by the addition of functional GroEL and GroES in a self-chaperoning process. Similarly, the assembly of Cpn60 oligomers was stimulated by GroES and other co-chaperonins were shown to have the same effect (Vitlin et al., 2011). Here, we have shown selective stimulation effects by GroES and SR-GroEL on assembly of oligomers containing CPN60β2. GroES likely directly interacts with Cpn60 oligomers in a manner similar to its interaction with GroEL. Indeed, CPN60 cooperated with GroES to rescue growth in the absence of GroES/EL function (Figure 6A and 6B). Similarly, SR-GroEL, which exposes the equatorial domain responsible for critical ring–ring interactions, may interact directly with the corresponding domain of

Subunits	Peptide	Ratio 1	Average	Number	Ratio 2	Average	Number	Overall
CPN60α	α-1	0.52796			0.31313			
	α-2	0.62903	0.60425	5.2	0.36245	0.35400	4.9	5
	α-3	0.65577			0.38632			
CPN60β1	β1-1	0.71756	0.65493	5.6	0.45336	0.41844	5.8	6
	β1-3	0.59230			0.38352			
CPN60β2	β2-1	0.35033	0.37583	3.2	0.21826	0.23426	3.3	3
	β2-2	0.40132			0.25026			

Table 3. Stoichiometry of Each Subunit within CPN60 Tetradecamer.

CPN60β2. We suspect that it is these interactions between either GroES or SR-GroEL and CPN60β2 that stabilize assembly intermediates that would otherwise disassemble.

Chloroplast Chaperonin Composition and Stoichiometry in Plants

Chloroplast chaperonin is encoded by multiple chaperonin genes divided into two distinct subunit types and therefore differs from the GroEL chaperonin, which is encoded by only one gene. Previous data suggest that the chloroplast chaperonin tetradecamer composed of hetero-oligomers of both Cpn60α and Cpn60β is the authentic native-state chaperonin complex functional in all plastids (Martel et al., 1990; Viitanen et al., 1995). However, the existence of small populations of functional homo-oligomers *in vivo* remained possible, especially since Cpn60β homo-oligomers reconstituted *in vitro* refold RrRubisco (Dickson et al., 2000; Vitlin et al., 2011). Furthermore, the observation of two distinct oligomers in chloroplast stroma extract suggested that at least two distinct types of chaperonin oligomers occur naturally in plastids (Nishio et al., 1999). Our data indicate that there might be only one hetero-oligomeric CPN60 chaperonin complex made up of all three subunits (i.e. CPN60αβ1β2) assembled into tetradecamers in *Chlamydomonas* chloroplasts. First, immunoprecipitation using whole-cell extracts yielded only one distinct chloroplast complex containing all three subunits (Figure 1C). A second complex was detected but it contained a mitochondrial subunit together with chloroplast subunits, likely an artifact of the cross-specificity of the antibody used, and not relevant *in vivo*. Second, the formation of CPN60β homo-oligomers was nearly abolished in the *E. coli* system by co-expressing other subunits (Figure 2A) and, similarly, CPN60β1 homo-oligomers were less prone to form when equimolar amounts of other subunits were present (Figure 4A). These results suggest that the affinity between different subunits is higher than that among the same subunits. Because the three CPN60 subunits are expressed to a similar level in *Chlamydomonas* (Thompson et al., 1995), it is likely that all subunits are equally abundant in the chloroplast, leading to competitive subunit interactions that favor hetero-oligomer rather than homo-oligomer formation. Homo-oligomers of individual subunits therefore likely do not play a significant functional role in the cell and, consistently, expression of individual CPN60 subunits was not able to complement a growth defect caused by a lack of GroEL in *E. coli* (Figure 6A).

We specifically attempted to detect other possible hetero-oligomers of CPN60α and CPN60β subunits (CPN60αβ1 and CPN60αβ2) but found that the levels of these hetero-oligomers were negligible (Figure 2A), although co-expression could complement GroEL function *in vivo* (Figure 6A). CPN60αβ1β2 oligomer, rather than homo-oligomers, physically and functionally interacts with co-chaperonin to refold substrate (Figure 5). For these reasons, we suggest that the CPN60αβ1β2 oligomer is the functional CPN60 complex in *Chlamydomonas* chloroplast. In *Arabidopsis*, Peng et al. (2011) detected five Cpn60 subunits out of six (Peng et al., 2011), and we detected all six subunits in chloroplast extracts (experimental observation), suggesting that all six subunits might be involved in the constitution of Cpn60 oligomers. It has long been thought that chloroplast Cpn60 consists of seven Cpn60α and seven Cpn60β subunits ($Cpn60\alpha_7\beta_7$) (Hemmingsen and Ellis, 1986; Martel et al., 1990; Bonk et al., 1996), however our subunit stoichiometry analyses indicate that the number of α type subunit was less, only five subunits in the functional tetradecamer (Figure 7A and Table 3). It is plausible that the subunit composition, stoichiometry, and molecular architecture of chloroplast chaperonins vary significantly among species. Since Cpn60 complexes undergo dynamic disassembly/assembly processes in the presence of ATP, it is also plausible that the subunit stoichiometry might differ under stress conditions.

Protomer Roles in the Functional Chaperonin Oligomer

Our analyses have also shed light on the individual roles of the CPN60 subunits. Assembly-prone $CPN60\beta1_{-M}$ readily formed oligomers upon exposure to ATP, while $CPN60\beta2_{-M}$ required a folding template such as SR-GroEL to promote its oligomerization (Figure 4). These results suggest that assembly-prone CPN60β1 may drive oligomerization upon ATP hydrolysis, with CPN60β2 playing a more minor role, being readily incorporated once presented with a template. CPN60α does not oligomerize on its own, even in the presence of ATP and SR-GroEL (Figure 4C), but it can be incorporated into the CPN60αβ1β2 oligomer. Its role may be to serve as a scaffold for the formation of the CPN60αβ1β2 complex. Our data support the notion that CPN60β1 may spontaneously initiate oligomerization in the ATP-rich environment of the chloroplast. In parallel, ATP-mediated disassembly of oligomers or other aberrant intermediates may serve as a quality control step-on pathway to the formation of functional chaperonin oligomers. Assembly intermediates likely interact with pre-existing factors with unique molecular architectures (such as those present in SR-GroEL and GroES) in an ATP-dependent manner, changing protomers or intermediates into assembly-competent forms, which are readily oligomerized into tetradecamers.

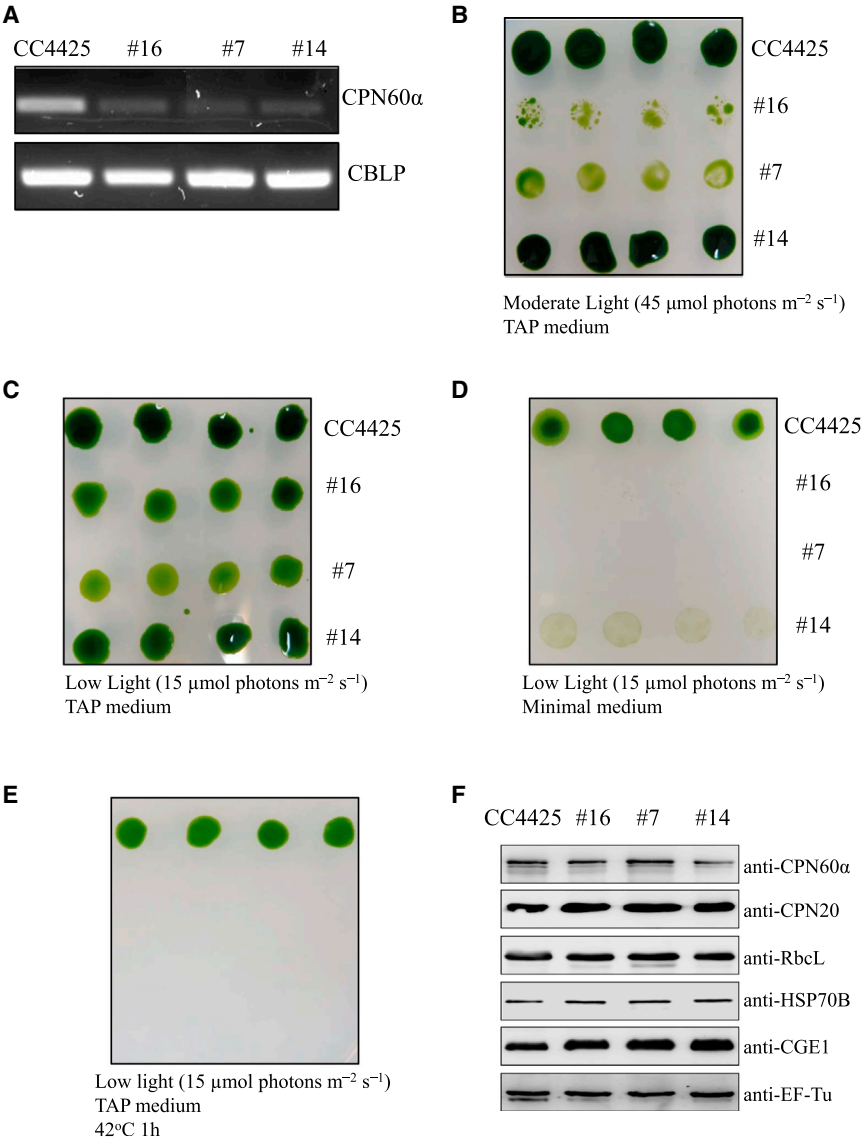

Figure 8. Down-Regulation of *CPN60α* in *Chlamydomonas*.

(A) CPN60α mRNA levels in *CPN60α* -amiRNAi strains are strongly reduced. 5 μg of whole-cell mRNA was used to do RT–PCR with specific primers of *CPN60α* gene and the PCR product was loaded on an agarose gel. CBLP served as a loading control.

(B and C) *CPN60α* -amiRNAi strains grew better at low light intensity (15 μmol photons m^{-2} s^{-1}) than at moderate light intensity (45 μmol photons m^{-2} s^{-1}). 10 μl of liquid TAP medium containing 10^7 cells was spotted onto TAP agar plates and grown for 2 weeks at the indicated light intensities.

(D) *CPN60α* -amiRNAi strains could not grow autotrophically. 10 μl of liquid TAP medium containing 10^7 cells was spotted onto minimal medium agar plates and grown for 1 week at low light intensities (15 μmol photons m^{-2} s^{-1}).

(E) *CPN60α* -amiRNAi strains could not grow after heat shock treatment. Liquid TAP medium containing 10^7 cells was incubated at 42°C for 1 h and spotted onto TAP agar plates, then grown for 1 week at low light intensities (15 μmol photons m^{-2} s^{-1}).

(F) Protein levels in *CPN60α* -amiRNAi strains. Whole-cell extract from wild-type and amiRNAi strains were separated on 12% SDS–PAGE and analyzed by immunoblotting with indicated serum.

CPN60β1 and CPN60β2 share high sequence homology and are functionally redundant in *E. coli* since either CPN60β subunit could cooperate with CPN60α to complement GroEL function (Figure 6A and 6B). Surprisingly, the co-presence of both CPN60β subunits could partially complement endogenous GroEL function *in vivo*, in contrast to either of the CPN60β subunits alone, suggesting that CPN60β subunits were also functionally diverse. The co-presence of CPN60α and one or two CPN60β subunits could fully complement endogenous GroEL function *in vivo* even under heat stress conditions (Figure 6A and 6B), suggesting that CPN60α is important to the chaperonin system, which is consistent with the lethal phenotype of the CPN60α insertion mutant in *Arabidopsis* and maize (Barkan, 1993; Suzuki et al., 2009; Feiz et al., 2012). In *Arabidopsis*, single insertion mutations in either of the CPN60α subunits led to retardation of plant embryo development, suggesting that the two CPN60α subunits were not functionally redundant and were indispensable to *Arabidopsis*. Meanwhile, single insertional mutations in CPN60β1 (At5g56500), CPN60β2, or CPN60β4 did not cause overt mutant phenotypes (Suzuki et al., 2009; Peng et al., 2011), while mutations in both CPN60β1 and CPN60β2 caused small albino seedlings, suggesting that the two subunits were functionally redundant. But each chloroplast CPN60 subunit may evolve to recognize specific substrates, e.g. NdhH was specifically folded by CPN60β4 (Peng et al., 2011) in *Arabidopsis* and GroEL obligate substrate was folded by CPN60 with specificity in our analysis (Figure 6C). Our CPN60α-amiRNA strains are defective in autotrophic photosynthesis (Figure 8) and serve as an important basis for future studies investigating the components of autotrophic photosynthesis that are impaired in CPN60α-amiRNA strains.

MATERIALS AND METHODS

Plasmids and Proteins

Plasmid construction of *CPN60α-pET11a*, *CPN60β1-pET11a*, *CPN60β2-pET11a*, *CPN60αβ1-pET11a*, *CPN60αβ2-pET11a*, *CPN60αβ1β2-pET11a*, *GroES-pET21*, *pOFX-groES-CrCPN60α*, *pOFX-groES-CrCPN60β1*, *pOFX-groES-CrCPN60β2*, *pOFX-groES-CrCPN60αβ1*, *pOFX-groES-CrCPN60αβ2*, *pOFX-groES-CrCPN60β1β2*, *pOFX-groES-CrCPN60αβ1β2*, and *CPN60αRNAi-pE383*, expression and purification of chaperonin complexes, chaperonin monomers, GroEL, GroES, and RrRubisco, and the production of antiserum are described in the Supplemental Experimental Procedures.

Soluble Protein, Native PAGE, and 2D SDS–PAGE

The extraction of soluble protein from *Chlamydomonas* cells, native PAGE, and two-dimensional (2D) SDS–PAGE were performed as

described previously (Liu et al., 2005) (see Supplemental Experimental Procedures for details).

Co-immunoprecipitation and Protein Identification by MS

Co-immunoprecipitation experiments were performed according to Liu et al. (2005) and detailed procedures are supplied in the Supplemental Experimental Procedures.

AFFFF–MALS

Protein complexes (1 mg/ml) were analyzed using the AFFFF system (Eclipse 3+; Wyatt Technology, Santa Barbara, CA) with a 350-mm spacer and 10-kDa RC membrane (Wyatt Technology) with elution flow of 1 ml/min and cross flow of 1.5 ml/min. The AFFFF device was connected to three successive detectors: a MALS detector (DAWN HELEOS II, 658 nm wavelength; Wyatt Technology), a 280-nm wavelength detector (1100 series; Agilent, Santa Clara, CA), and differential refractive index detector (dRI) (Optilab rEX, 658 nm; Wyatt Technology). Molar masses were calculated using the ASTRA 5 software (Wyatt Technology) with Dn/dc values set to 0.185 ml/g for protein.

PK Digestion Assay

The PK digestion assay was performed in buffer A (20 mM MOPS/KOH [pH 7.5], 100 mM KCl, 5 mM $Mg(OAc)_2$) containing 0.5 μg/μl chaperonin complexes, followed by the addition of the indicated amount of PK (from *Tritirachium album*; Roche, Basel, Switzerland) and incubation for 30 min at 25°C; PK was stopped with 1 mM phenylmethylsulfonyl fluoride. Reactions were analyzed with 10% SDS–PAGE followed by Coomassie staining.

ATPase Assay

A coupled enzymatic assay was used and the ATPase activity was monitored based on the absorbance of NADH at 340 nm. The reaction mixture contained 20 mM MOPS/KOH (pH 7.5), 100 mM KCl, 10 mM $MgCl_2$, 1 mM phosphoenolpyruvate, 20 units pyruvate kinase/ml, 30 units lactate dehydrogenase/ml, 0.25 mM NADH, and 1 mM ATP, with or without 0.5 μM co-chaperonin; absorbance at 340 nm was monitored immediately after the addition of 0.2 μM chaperonin oligomer or 1.4 μM chaperonin monomer.

Reconstitution of CPN60 Oligomers from Protomers

The reconstitution experiments were performed in buffer A containing a total of 0.45 mg/ml chaperonin protomers with 5 mM DTT, 4 mM ATP or ADP or 0.25 mg/ml co-chaperonin GroES, as indicated in the figures. The reaction mixture was incubated for 5 min at room temperature and then for 1 h at 30°C. Samples were then loaded on 5%–13% gradient colorless native PAGE and visualized by Coomassie staining.

Pull-Down Assay

A total of 100 μg of $GroES_{6His}$ was immobilized to Ni-NTA beads and incubated with 50 μg of GroEL or CPN60 oligomers for 4 h at 25°C in buffer containing 20 mM Tris–HCl (pH 7.5), 2.5 mM $Mg(OAc)_2$, 7.5 mM $MgCl_2$, 20 mM KCl, and 80 mM NaCl, supplied with 1 mM ATP or ADP. Beads were washed three times with the above buffer plus 40 mM imidazole and 0.1 mM respective nucleotides. Proteins were eluted with 50 μl of extraction buffer plus 1 M imidazole, and 10 μl of the samples was resolved by denaturing SDS–PAGE and visualized by Coomassie staining.

Rubisco Refolding Assay

Recombinantly purified Rubisco of *Rhodospirillum rubrum* was denatured in buffer A with 10 mM DTT and 6 M guanidinium hydrochloride for 1 h at 25°C and then diluted 100-fold into ice-cold assay buffer A containing 5 mM DTT with or without 1 μM GroEL or CPN60 oligomers. The reaction mixture was incubated for 5 min at 25°C and centrifuged for 10 min at 16 100 *g* at 4°C. The supernatant was transferred into new tubes and supplied with 1 mg/ml bovine serum albumin and 1 μM co-chaperonin. Refolding was initiated with 2 mM ATP and the reaction was stopped with 10 mM glucose and 2.5 U of hexokinase. The reaction was loaded on 5%–13% native gel and immunodetected with Rubisco serum.

Complementation of GroEL Function by CPN60

E. coli MGM100 competent cells, purchased from the *E. coli* Genetic Stock Center, Yale (http://cgsc.biology.yale.edu/), were prepared using a standard procedure and were transformed with pOFX-GroE or pOFX-CPN60 plasmids by electroporation with a MicroPulser™ Electroporation apparatus from Bio-Rad. The transformants were selected and a single colony was grown in LB medium with kanamycin and spectinomycin, supplemented with 0.02% arabinose. One milliliter of cells was collected after the culture grew to an OD_{600} of approximately 1, and the cells were washed four to five times with 1 ml of LB. The harvested cells were resuspended in 1 ml of LB and ten-fold serial dilutions were made up to a dilution of 10^{-7}. A volume of 7.5 μl was then spotted onto an LB agar plate with the relevant antibiotics, supplemented with arabinose, glucose, or glucose/IPTG to grow either at 37°C or 42°C for 15 h.

Solubility Analysis of GroEL Obligate Substrates

MGM100 cells containing *pOFX-GroE* or *pOFX-CPN60* plasmids were transformed with *DapA-pLCM2*, *HemB-pLCM2*, and *MetK-pLCM2* and were grown on the medium plate with ampicillin, spectinomycin, and kanamycin resistances. A single colony was picked to grow in the LB medium with 0.02% arabinose supplemented to an OD_{600} of 0.6. The cells were collected and washed five times with LB and allowed to grow from an OD_{600} of 0.01 in LB supplemented with 1 mM Diaminopimelic acid (DAP), 0.2% glucose to an OD_{600} of 0.1. The chaperonin was then induced with the addition of 1 mM IPTG for 0.5 h followed by addition of 50 ng/ml Tet to induce expression of substrates for 2 h. The cells were collected and fractionated by centrifugation following sonication. The total cell lysate and the soluble fraction of the proteins derived from the cell lysate were loaded on the gel and analyzed with SDS–PAGE followed by Coomassie staining.

CPN60-QconCAT Protein Expression and Purification

The CPN60-QconCAT gene encoding selected CPN60 peptides (Table 2) was synthesized with two additional peptides as described by Pratt et al. (2006) with minor modifications. The gene was cloned into expression vector pET22b with *NdeI* and *HindIII* sites, resulting in the CPN60-QconCAT-pLCM2 encoding protein with a C-terminal His6 tag. The full CPN60-QconCAT protein sequence is found in the Supplemental Information. The plasmid was then transformed into BL21DE3 cells and the cells were grown in minimal medium with an amino acid mixture containing L-[$^{13}C_6$]-Lys and L-[$^{13}C_6$]-Arg (97%–99% enrichment; Cambridge Isotope Laboratories). The protein was induced with 1 mM IPTG at an OD of 0.6 for 4 h and was further purified with a standard procedure (details of the procedure are given in the Supplemental Information).

Quantitative LC-MS/MS Analysis and Data Processing

The purified CPN60-QconCAT labeled with isotope and CPN60αβ1β2 proteins was digested with trypsin as described (Wisniewski et al., 2009). The digested peptides were then analyzed on a Q Exactive (Thermo Scientific) equipped with an Easy-nLC 1000 HPLC system (Thermo Scientific). The peptides were loaded onto a fused silica trap column (100 μm inner diameter × 2 cm) packed in-house with reversed-phase silica (Reprosil-Pur C18 AQ, 5 μm; Dr. Maisch GmbH) and then separated on a C18 column (75 μm inner diameter × 20 cm) packed with reversed-phase silica (Reprosil-Pur C18 AQ, 3 μm; Dr. Maisch GmbH). The peptides bound on the column were eluted with a 58-min linear gradient of acetonitrile solution containing 0.1% formic acid. The eluted peptides were analyzed with a Q Exactive mass spectrometer (Thermo Scientific). Using data-dependent acquisition mode, the MS data were acquired at a high resolution of 70 000 (*m/z* 200) across the mass range of 300–1600 *m/z*. The target value was 3.00e+06 with a maximum injection time of 60 ms. The top 20 precursor ions were selected from each MS full scan with an isolation width of 2 *m/z* for fragmentation in

the HCD collision cell with normalized collision energy of 27%. Subsequently, MS/MS spectra were acquired at a resolution of 17 500 at *m/z* 200. The target value was 5.00e+04 with a maximum injection time of 80 ms. The dynamic exclusion time was 40 s. For nanoelectrospray ion source setting, the spray voltage was 2.0 kV; no sheath gas flow; the heated capillary temperature was 320°C. The MS/MS data were analyzed with Proteome Discovery version 1.4 using the Sequest HT search engine for protein identification and Percolator for the false discovery rate (FDR) against a UniProt human protein database (updated in June, 2013). FDR analysis was performed with Percolator and FDR <1% was set for protein identification. The peptide confidence was set to high for the peptide filter.

Down-Regulation of CPN60α in *Chlamydomonas*

The *Chlamydomonas* strain CC4425 (*cw15 nit2-203 mt+*), obtained from the *Chlamydomonas* Genetic Center (http://www.chlamy.org/), was grown mixotrophically in TAP medium to about 4 × 10^6 cells/ml with continuous light (45 μmol photons m^{-2} s^{-1}) at 23°C. Then the cells were collected and transformed with linearized CPN60αRNAi-pE383 using a glass beads procedure as described by Kindle (1990). Transformants were selected on TAP medium supplemented with 10 μg/ml paromomycin under low light (15 μmol photons m^{-2} s^{-1}) for 7–15 days.

SUPPLEMENTAL INFORMATION

Supplemental Information is available at *Molecular Plant Online*.

FUNDING

This work was supported by "One-hundred talents" Startup Funds from the Chinese Academy of Sciences and funded by the State Key Laboratory of Plant Cell and Chromosome Engineering (grant no: PCCE-2012-TD-01).

AUTHOR CONTRIBUTIONS

C.B. executed most of the experiments. P.G. carried out the *in vivo* experiments and CPN60 refolding ability analysis. Q.Z. performed the amiRNAi experiments. Z.L. performed the pull-down experiments, purified the CPN60αβ1β2 oligomers, and did the sequence alignment. S.Z. and F.G. contributed to plasmid construction. L.G. and Y.W. performed mass spectrometry identification. Z.T. was involved in the data analysis and interpretation of the results. J.W and F.Y performed the quantitative mass spectrometry. C.L. supervised the design and interpretation of the biochemical experiments and wrote the manuscript.

ACKNOWLEDGMENTS

We thank Dr. Manajit Hayer Hartl and Prof. Franz Ulrich Hartl for their generous gifts of plasmids containing groEL, groEL-SR, groES, and RrRubisco, Dr. Olivier Fayet for his kind gift of plasmid pOFX-GroE, Prof. Kaiyao Huang for his kind gift of plasmid pHK85, Prof. Michael Schroda for his kind gift of HSP70B and CGE1 serum. We would like to thank Dr. Sarah Schäuffelhut and Prof. Weicai Yang for their critical reading of the manuscript. No conflict of interest declared.

Received: March 30, 2015
Revised: May 10, 2015
Accepted: June 3, 2015
Published: June 6, 2015

REFERENCES

Barkan, A. (1993). Nuclear mutants of maize with defects in chloroplast polysome assembly have altered chloroplast RNA metabolism. Plant Cell **5**:389–402.

Bonk, M., Tadros, M., Vandekerckhove, J., Al-Babili, S., and Beyer, P. (1996). Purification and characterization of chaperonin 60 and heat-shock protein 70 from chromoplasts of *Narcissus pseudonarcissus*. Plant Physiol. **111**:931–939.

Booth, C.R., Meyer, A.S., Cong, Y., Topf, M., Sali, A., Ludtke, S.J., Chiu, W., and Frydman, J. (2008). Mechanism of lid closure in the eukaryotic chaperonin TRiC/CCT. Nat. Struct. Mol. Biol. **15**:746–753.

Castanie, M.P., Berges, H., Oreglia, J., Prere, M.F., and Fayet, O. (1997). A set of pBR322-compatible plasmids allowing the testing of chaperone-assisted folding of proteins overexpressed in *Escherichia coli*. Anal. Biochem. **254**:150–152.

Dickson, R., Weiss, C., Howard, R.J., Alldrick, S.P., Ellis, R.J., Lorimer, G., Azem, A., and Viitanen, P.V. (2000). Reconstitution of higher plant chloroplast chaperonin 60 tetradecamers active in protein folding. J. Biol. Chem. **275**:11829–11835.

Feiz, L., Williams-Carrier, R., Wostrikoff, K., Belcher, S., Barkan, A., and Stern, D.B. (2012). Ribulose-1,5-bis-phosphate carboxylase/oxygenase accumulation factor1 is required for holoenzyme assembly in maize. Plant Cell **24**:3435–3446.

Fujiwara, K., Ishihama, Y., Nakahigashi, K., Soga, T., and Taguchi, H. (2010). A systematic survey of in vivo obligate chaperonin-dependent substrates. EMBO J. **29**:1552–1564.

Hartl, F.U., Bracher, A., and Hayer-Hartl, M. (2011). Molecular chaperones in protein folding and proteostasis. Nature **475**:324–332.

Hayer-Hartl, M.K., Martin, J., and Hartl, F.U. (1995). Asymmetrical interaction of GroEL and GroES in the ATPase cycle of assisted protein folding. Science **269**:836–841.

Hemmingsen, S.M., and Ellis, R.J. (1986). Purification and properties of ribulosebisphosphate carboxylase large subunit binding protein. Plant Physiol. **80**:269–276.

Hill, J.E., and Hemmingsen, S.M. (2001). *Arabidopsis thaliana* type I and II chaperonins. Cell Stress Chaperones **6**:190–200.

Horwich, A.L., Farr, G.W., and Fenton, W.A. (2006). GroEL-GroES-mediated protein folding. Chem. Rev. **106**:1917–1930.

Horwich, A.L., Fenton, W.A., Chapman, E., and Farr, G.W. (2007). Two families of chaperonin: physiology and mechanism. Annu. Rev. Cell Dev. Biol. **23**:115–145.

Hu, J., Deng, X., Shao, N., Wang, G., and Huang, K. (2014). Rapid construction and screening of artificial microRNA systems in *Chlamydomonas reinhardtii*. Plant J. **79**:1052–1064.

Kerner, M.J., Naylor, D.J., Ishihama, Y., Maier, T., Chang, H.C., Stines, A.P., Georgopoulos, C., Frishman, D., Hayer-Hartl, M., Mann, M., et al. (2005). Proteome-wide analysis of chaperonin-dependent protein folding in *Escherichia coli*. Cell **122**:209–220.

Kim, S., Willison, K.R., and Horwich, A.L. (1994). Cytosolic chaperonin subunits have a conserved ATPase domain but diverged polypeptide-binding domains. Trends Biochem. Sci. **19**:543–548.

Kindle, K.L. (1990). High-frequency nuclear transformation of *Chlamydomonas reinhardtii*. Proc. Natl. Acad. Sci. USA **87**:1228–1232.

Koumoto, Y., Shimada, T., Kondo, M., Takao, T., Shimonishi, Y., Hara-Nishimura, I., and Nishimura, M. (1999). Chloroplast Cpn20 forms a tetrameric structure in *Arabidopsis thaliana*. Plant J. **17**:467–477.

Leitner, A., Joachimiak, L.A., Bracher, A., Monkemeyer, L., Walzthoeni, T., Chen, B., Pechmann, S., Holmes, S., Cong, Y., Ma, B., et al. (2012). The molecular architecture of the eukaryotic chaperonin TRiC/CCT. Structure **20**:814–825.

Lissin, N.M., Venyaminov, S., and Girshovich, A.S. (1990). (Mg-ATP)-dependent self-assembly of molecular chaperone GroEL. Nature **348**:339–342.

Liu, C., Willmund, F., Whitelegge, J.P., Hawat, S., Knapp, B., Lodha, M., and Schroda, M. (2005). J-domain protein CDJ2 and HSP70B are a plastidic chaperone pair that interacts with vesicle-inducing protein in plastids 1. Mol. Biol. Cell **16**:1165–1177.

Martel, R., Cloney, L.P., Pelcher, L.E., and Hemmingsen, S.M. (1990). Unique composition of plastid chaperonin-60: alpha and beta polypeptide-encoding genes are highly divergent. Gene **94**:181–187.

McLennan, N., and Masters, M. (1998). GroE is vital for cell-wall synthesis. Nature **392**:139.

Nishio, K., Hirohashi, T., and Nakai, M. (1999). Chloroplast chaperonins: evidence for heterogeneous assembly of alpha and beta Cpn60 polypeptides into a chaperonin oligomer. Biochem. Biophys. Res. Commun. **266**:584–587.

Nordhues, A., Schottler, M.A., Unger, A.K., Geimer, S., Schonfelder, S., Schmollinger, S., Rutgers, M., Finazzi, G., Soppa, B., Sommer, F., et al. (2012). Evidence for a role of VIPP1 in the structural organization of the photosynthetic apparatus in *Chlamydomonas*. Plant Cell **24**:637–659.

Olinares, P.D., Kim, J., Davis, J.I., and van Wijk, K.J. (2011). Subunit stoichiometry, evolution, and functional implications of an asymmetric plant plastid ClpP/R protease complex in *Arabidopsis*. Plant Cell **23**:2348–2361.

Peng, L., Fukao, Y., Myouga, F., Motohashi, R., Shinozaki, K., and Shikanai, T. (2011). A chaperonin subunit with unique structures is essential for folding of a specific substrate. PLoS Biol. **9**:e1001040.

Pratt, J.M., Simpson, D.M., Doherty, M.K., Rivers, J., Gaskell, S.J., and Beynon, R.J. (2006). Multiplexed absolute quantification for proteomics using concatenated signature peptides encoded by QconCAT genes. Nat. Protoc. **1**:1029–1043.

Schroda, M. (2004). The Chlamydomonas genome reveals its secrets: chaperone genes and the potential roles of their gene products in the chloroplast. Photosynth. Res. **82**:221–240.

Suzuki, K., Nakanishi, H., Bower, J., Yoder, D.W., Osteryoung, K.W., and Miyagishima, S.Y. (2009). Plastid chaperonin proteins Cpn60 alpha and Cpn60 beta are required for plastid division in *Arabidopsis thaliana*. BMC Plant Biol. **9**:38.

Thompson, M.D., Paavola, C.D., Lenvik, T.R., and Gantt, J.S. (1995). *Chlamydomonas* transcripts encoding three divergent plastid chaperonins are heat-inducible. Plant Mol. Biol. **27**:1031–1035.

Tsai, Y.C., Mueller-Cajar, O., Saschenbrecker, S., Hartl, F.U., and Hayer-Hartl, M. (2012). Chaperonin cofactors, Cpn10 and Cpn20, of green algae and plants function as hetero-oligomeric ring complexes. J. Biol. Chem. **287**:20471–20481.

Viitanen, P.V., Schmidt, M., Buchner, J., Suzuki, T., Vierling, E., Dickson, R., Lorimer, G.H., Gatenby, A., and Soll, J. (1995). Functional characterization of the higher plant chloroplast chaperonins. J. Biol. Chem. **270**:18158–18164.

Vitlin, A., Weiss, C., Demishtein-Zohary, K., Rasouly, A., Levin, D., Pisanty-Farchi, O., Breiman, A., and Azem, A. (2011). Chloroplast beta chaperonins from *A. thaliana* function with endogenous cpn10 homologs in vitro. Plant Mol. Biol. **77**:105–115.

Wisniewski, J.R., Zougman, A., Nagaraj, N., and Mann, M. (2009). Universal sample preparation method for proteome analysis. Nat. Methods **6**:359–362.

Xu, Z.H., Horwich, A.L., and Sigler, P.B. (1997). The crystal structure of the asymmetric GroEL-GroES-(ADP)(7) chaperonin complex. Nature **388**:741–750.